

Atomic force microscopy images of lyotropic lamellar phases

C. Garza, L. T. Thieghi, and R. Castillo^{a)}

*Instituto de Física, Universidad Nacional Autónoma de México, P.O. Box 20-364,
D. F. México, 01000 México*

(Received 4 December 2006; accepted 11 January 2007; published online 7 February 2007)

For the very first time, atomic force microscope images of lamellar phases were observed combined with a freeze fracture technique that does not involve the use of replicas. Samples are rapidly frozen, fractured, and scanned directly with atomic force microscopy, at liquid nitrogen temperature and in high vacuum. This procedure can be used to investigate micro-structured liquids. The lamellar phases in Sodium bis(2-ethylhexyl) sulfosuccinate (AOT)/water and in $C_{12}E_5$ /water systems were used to assess this new technique. Our observations were compared with x-ray diffraction measurements and with other freeze fracture methods reported in the literature. Our results show that this technique is useful to image lyotropic lamellar phases and the estimated repeat distances for lamellar periodicity are consistent with those obtained by x-ray diffraction. © 2007 American Institute of Physics. [DOI: 10.1063/1.2483389]

INTRODUCTION

When amphiphiles are dissolved in a liquid, they self-assemble to make aggregates of molecules or supramolecular structures. Depending on the thermodynamic conditions and amphiphile geometry (packing parameter), amphiphiles can arrange themselves in different configurations,¹ like spherical micelles, reverse micelles, cylindrical micelles, bilayers, bi-continuous structures, etc. Lyotropic lamellar phases, L_α , are formed by infinite bilayers of surfactant molecules, flat on the average, which are stacked periodically and parallel to each other, with a regular interlayer spacing, d , forming a structure similar to that of a smectic A thermotropic liquid crystal. These solutions present quite remarkable physical properties, as being rather fluid and transparent as observed with natural light. However, when viewed in polarized light, they are lit up by bright birefringent colors, revealing the large scale orientational order. Neutron and x-ray diffraction takes into account this order producing defined Bragg peaks at $q=2\pi/d$, which can be related to the amphiphile volume fraction, φ , and the bilayer thickness, δ , using $q=2\pi\varphi/\delta$.²

To elucidate complex fluid liquid microstructures, there are four techniques related to freeze fracture, namely, the freeze fracture electron microscopy (FFEM),^{3,4} the direct imaging of vitrified thin films named cryo-transmission electron microscopy (cryo-TEM),⁵ the freeze fracture direct imaging (FFDI),⁶ which is a hybrid of the previous mentioned techniques, and the freeze fracture scanning tunneling microscopy (FFSTM).⁷ These techniques owe their development to the introduction of controlled methods for equilibrating specimens prior to plunge vitrification, rationalization of the freezing process, and the identification of best cryogens.^{8,9} In FFEM, the liquid specimens are rapidly frozen, fractured, and shadowed with a metal, which is coated with a carbon

film to prevent metal oxidation. The metal replica of the fracture surface containing the morphology of the microstructure is viewed in a transmission electron microscope. In contrast, in cryo-TEM the frozen specimens are not replicated but immediately transferred to a low-temperature stage within the microscope and imaged directly. Both methods have advantages and disadvantages. In FFEM, if the system can be fractured, the kind of observed fractures are usually the cohesive ones, i.e., fractures through the bulk of the microemulsion, in contrast to adhesive fractures at the metal-microemulsion interface.⁶ In cryo-TEM, the electron beam damages the sample, which is particularly severe in the presence of water and even more in vitrified specimens that contain significant amounts of organic compounds. Another problem is related to the control of the film thickness, because the film has to be thin enough to allow direct imaging, but it has to be thick enough not to influence the microstructure.⁶ Although, there are techniques used to circumvent these problems,⁶ like blotting the sample prior to vitrification, the preparation of cryo-sections of vitrified samples, and the preparation of films where thickness is controlled interferometrically before vitrification, all of them are not free of problems and complications.⁹ FFDI is a hybrid technique where the sample is also freeze-fractured. However, instead of replicating the fracture, the fracture itself is observed by the microscope. This is done forming liquid films spanning the holes of a holey carbon film supported on a copper grid. A way to get the thin liquid films ready for TEM is to place the grid between two covering copper plates and to immerse this sandwich assembly into the liquid under study, where capillary forces make sure that the liquid penetrates the sandwich; covering plates protect samples from the cryogen. Afterwards, the assembly with the sample is precooled, frozen in liquid nitrogen, and fractured, then the grid is mounted in a cryo-holder and observed in the microscope.⁶ Electron microscopy examination has advantages related to the simplicity of imaging replicas at all

^{a)}Author to whom correspondence should be addressed. Electronic mail: rolandoc@fisica.unam.mx

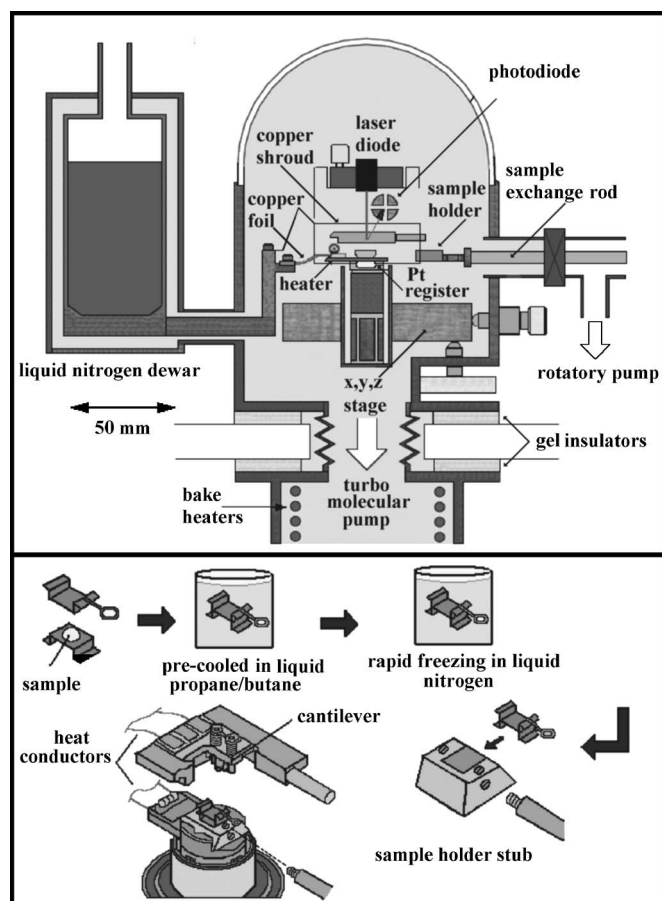


FIG. 1. (a) Cross section of the scanning probe microscope (head), scanner, and sample holder cooled through copper foils which are connected to a liquid nitrogen Dewar, all of them are inside of a vacuum chamber. (b) Cartoon showing the main steps for obtaining the frozen sample to be transferred into the microscope, where it will be fractured and scanned at liquid nitrogen temperature and at high vacuum. Figure has been modified from Ref. 12.

magnifications, as well as the ability to re-examine replicas. In FFSTM, high resolution and three dimensional images of structured fluids have been obtained using a freeze fracture replication method similar to those mentioned above. Although here, the sample replicas are directly imaged with a scanning tunneling microscope.⁷

The aim of this communication is to present a different procedure to image lamellar phases, which could be of help to investigate microstructured liquids; we named it freeze fracture atomic force microscopy (FFAFM). Here, liquid samples are rapidly frozen, fractured, and scanned directly with atomic force microscopy, at liquid nitrogen temperature and in high vacuum. To assess the capability of this new technique, we imaged well known lamellar phases, as those found in the systems AOT/water and $C_{12}E_5$ /water.¹⁰ Our observations were compared with x-ray diffraction measurements and with other freeze fracture methods combined with TEM reported in the literature. This procedure can be used to investigate the microstructure of a complex fluid, since the procedure is not complicated and AFM facilities with vacuum and low temperature are becoming quite common in research labs.

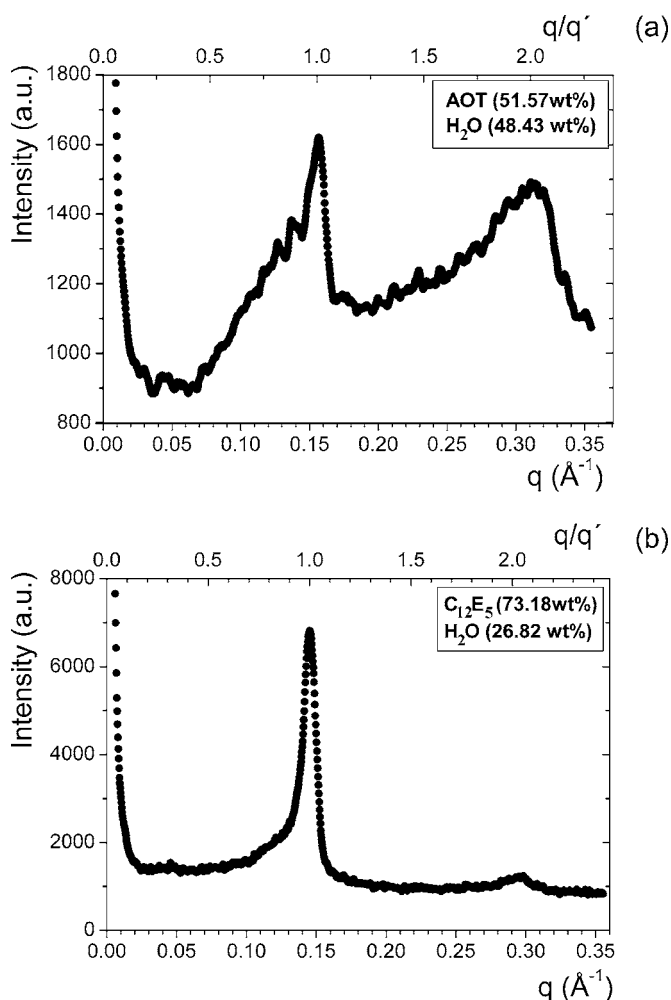


FIG. 2. Results of x-ray diffraction at low angles for the AOT/water system (a) and for the $C_{12}E_5$ /water system (b).

EXPERIMENTAL SECTION

Materials

Pentaethylene glycol monododecyl ether ($C_{12}E_5$, >98 wt.%) from Bio Chemika, Fluka Chemie (Germany) and Sodium bis(2-ethylhexyl) sulfosuccinate (AOT, 98 wt.%) from Aldrich Chem. Co. (WI) were used without further purification. Water was milli-Q water (Nanopure-UV, U.S.A. 18.3 M Ω). All measurements were made at least two weeks after the solution preparation to allow them to reach equilibrium. Solutions in the phases of interest here ($C_{12}E_5$ 73 wt.% /H₂O and AOT 51 wt.% /H₂O) were prepared by weight, mixing them with a vortex and using an ultrasound bath to homogenize them.

Apparatus: X ray diffraction

Diffraction measurements were carried out in a small-angle x-ray scattering (SAXS) instrument at room temperature using an x-ray generator (model RMN3kW, Rigaku, Japan) with a standard Cu K_{α} radiation. The generator was operated at 40 kV and 40 mA, and data were collected with a position-sensitive proportional counter detector (model 931129A02, Rigaku, Japan) using 2048 channels, sample-to-detector distance was set to 28.65 cm. The range of scatter-

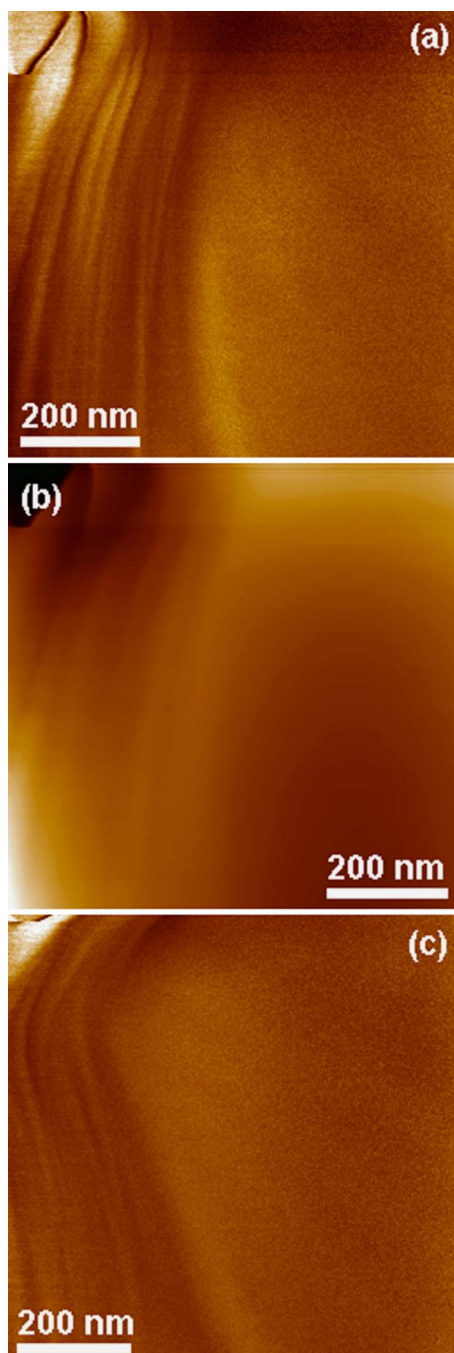


FIG. 3. Stack of flat surfaces obtained from frozen specimens of the AOT/water system with AFM. (a) and (c) Phase lag images. (b) Topographic image.

ing vector, $q = (4\pi/\lambda)\sin\theta$ (where 2θ is the scattering angle) was between 0.020 – 0.35 \AA^{-1} . The structure of lamellar phases was determined from the relative positions of the diffraction peaks. For a lamellar structure, the peaks position should obey the relation $1:2:3:4\dots$.¹¹ The interlayer spacing d of the lamellar structure was obtained from the position for the first diffraction peak, $q' = 2\pi/d$.

Atomic force microscopy

Freeze fractured specimens were scanned with a scanning probe microscope (JSTM-4200 JEOL, Japan) with a $25 \times 25 \mu\text{m}$ scanner which has an integrated vacuum system

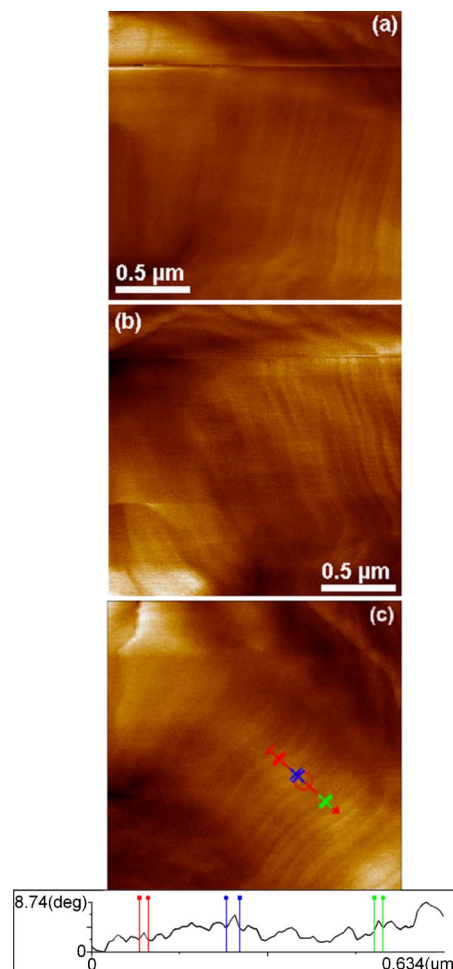


FIG. 4. Three phase lag images corresponding to specimens of the AOT/water system where the AFM scanning was made at different angles around the same area (from top to bottom: 30° , 60° , and 0° , respectively). In (c), measurements for different bands which can be observed in the vertical profile (distance between crosses, red: 16 nm ; blue: 24 nm ; and green: 15 nm).

(better than $1 \times 10^{-4} \text{ Pa}$) and a freeze fracture device inside the vacuum chamber (see Fig. 1). The AFM head contains a laser diode, a four-quadrant photodiode, a piezo scanner mounted in a XYZ coarse alignment stage, and a preamplifier, all of them located inside the vacuum chamber. The cantilever's deflection is detected using standard optical beam bounce technique and the laser can be aligned before evacuation. Vacuum evacuation is performed with a 300 l/s magnetic turbo molecular pump and a rotatory pump. Isolators between the turbomolecular pump and the chamber isolate the AFM from the pump vibrations. A copper cold finger coupled to a liquid nitrogen Dewar is mounted in the AFM chamber. The sample stage can be cooled via a heat conductor fabricated from ultra pure copper foils, where one end of the heat conductor is connected to the sample stage while the other end is coupled to the cold finger, the foils also decouple vibrations coming from the N_2 boiling. The temperature of the sample stage can be monitored by a platinum thin film resistor. The sample holder is thermally isolated from the piezo tube by an epoxy pillar heat shield. To prevent surface contamination due to the residual gas adsorption, a gold coated copper shroud is mounted around the sample holder.

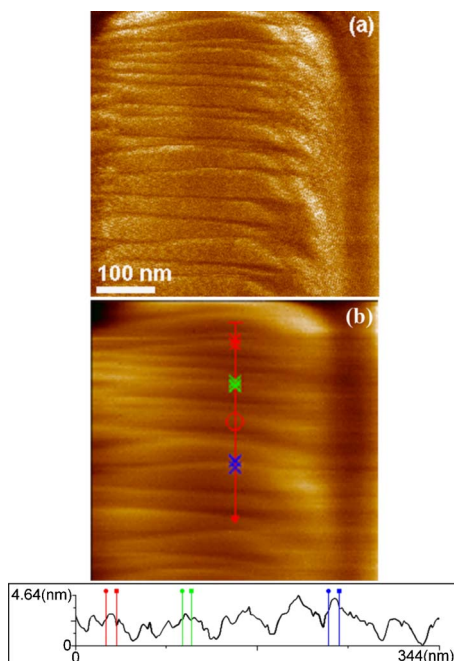


FIG. 5. Lamellar phase AFM images for a freeze fractured specimen of the $C_{12}E_5$ /water system. (a) Phase lag image. (b) Topographic image with measurements for different bands which can be observed in the vertical profile (distance between crosses, red: 9.45 nm; blue: 10.1 nm; and green: 8.78 nm).

The end of the copper shroud is coupled to the cooled cold finger. For inserting the sample and make the fracture, the instrument has an extension ring with a specimen exchange device that allows introducing a specimen rod with a sample holder without breaking the vacuum.¹²

Noncontact dynamic mode (intermittent contact) was used to obtain topographic and phase lag images of the samples. Noncontact silicon cantilevers with a typical force constant of 40 Nm^{-1} (Mickomash, OR) were used. Previous to each sample measurement, calibration was checked using calibrated gratings (Mickomash, OR) in vacuum and at liquid nitrogen temperature.

Sample preparation and freeze fracturing procedure

A small drop of a lamellar phase was deposited in a thin copper sample holder, previously cleaned with dilute nitric acid, and squeezed with a thin copper plate acting as a covering cap [see Fig. 1(b)]. This assembly with the sample is precooled with a liquid propane/butane mixture and afterwards it is submerged in liquid nitrogen where it is fastened to a sample holder stub. This stub is transferred into the sample stage in the AFM vacuum chamber using the sample exchange rod with a screw at the end. The sample is fractured with the sample exchange rod pulling upward the covering cap of the squeezed and frozen liquid. The exposed surface is scanned with a scanning probe microscope using intermittent contact mode. We ensured the instrument capability to reach atomic resolution measuring the interplanar distance along the [100] direction for a gold thin film. Our measured interplanar distance was $4.1 \pm 0.7 \text{ \AA}$ from the inverse fast Fourier transform coming from force images, this value is in agreement with the diffraction value of 4.078 \AA .¹³

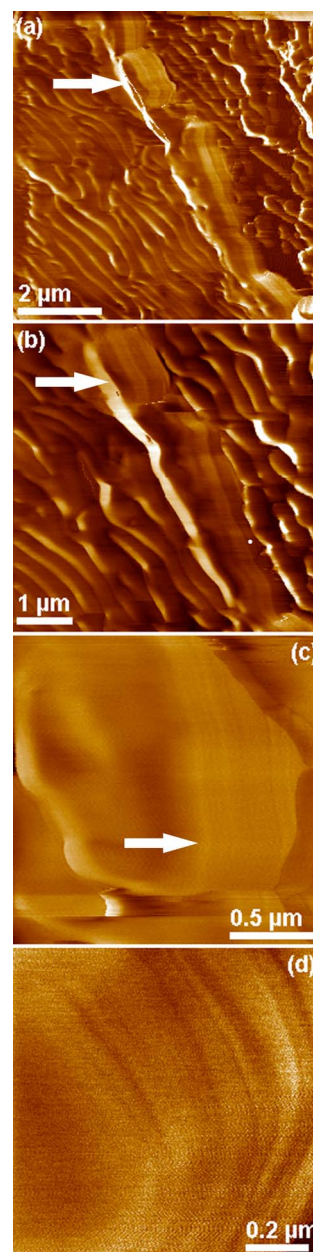


FIG. 6. Lamellar phase AFM images for a freeze fractured specimen of the $C_{12}E_5$ /water system showing, from top to bottom, different magnifications of a specific area indicated by an arrow.

RESULTS

Lamellar phases were prepared for two systems well known for their capability to form lamellar phases: AOT (51.57 wt. %)/water and $C_{12}E_5$ (73.18 wt. %)/water. These phases show birefringence and the lamellar interlayer spacing was determined using x-ray diffraction at low angles. Diffraction patterns, with second order peaks obeying the relation 1:2, are presented in Fig. 2. The lamellar interlayer spacing, d , is $43.3 \pm 0.3 \text{ \AA}$ for the $C_{12}E_5$ /water system and $40.4 \pm 0.3 \text{ \AA}$ for the AOT/water system, both in agreement with the values found in the literature.^{14,15}

The layered structure of lyotropic lamellar phases can be observed in Figs. 3–6 with the use of AFM in intermittent contact mode, i.e., the probe oscillates in resonance and touches the surface periodically, thus minimizing the friction

force. Image treatment was kept to a minimum, just a plane correction and an adjustment for brightness and contrast to whole images were done. In Figs. 3 and 4, we present images for the lamellar phase of the AOT/water system and in Figs. 5 and 6 we show images for the C₁₂E₅/water system. These images show ordered bands consistent with stacks of locally flat surfaces forming a layered structure as it would be expected for a lyotropic lamellar phase. Consecutive amplifications for checking the right amplification of image features, as well as scanings at different angles were done to avoid images with artifacts. This can be observed in Figs. 4 and 6. AFM images give a different point of view from those images obtained using TEM freeze fracture techniques for the same systems of interest here, as is shown in Figs. 3(a) and 3(b) from Ref. 10. For both systems, we present typical vertical profiles coming from topographic or phase lag images, where the thickness of the bands corresponding to stacks of several bilayers can be obtained. Usually, it is not possible to observe bands of a thickness similar to the interlayer spacing d given by x-ray diffraction, since roughness in the fractured sample did not allow reaching molecular resolution. However, band thickness must be a multiple of d . To test this, band thickness measurements were divided by rough estimates for d^{est} obtained from $d^{\text{est}} = \delta/\varphi$; δ can be estimated from the geometry of the surfactant. For each measured band, we modified the estimated repeat distance accordingly to obtain an entire multiple when band thickness was divided by these modified repeat distances. When these modified d^{est} values are averaged over a large number of band measurements, we obtain a repeat distance of $d = 40.4 \pm 0.8 \text{ \AA}$ and of $d = 43.7 \pm 0.8 \text{ \AA}$ for the AOT/water system and for the C₁₂E₅/water system, respectively, well in agreement with the interlayer spacing d value obtained with x-ray diffraction.

In summary, we have employed a new and useful technique using an atomic force microscope for studying microstructure in complex fluids, where a fracture in a frozen liquid sample can be observed *in situ*, avoiding artifacts, which are common when metal replicas are done. In addition, fro-

zen samples are not damaged during the observation due to exposure of the sample to the electron beam. FFAFM gives approximately the same lateral resolution as those techniques related to electron microscopy, but here direct measurements of vertical topography can be obtained instead of inferring them as in TEM. There is also the possibility of studying local composition using phase lag or contact analysis. With FFAFM, we were able to observe lyotropic lamellar phases and as far as we know, it is the first time where the microstructure of these phases has been observed directly. Furthermore, the interlayer spacing measured on vertical profiles is consistent with the interlayer spacing obtained by x-ray diffraction.

ACKNOWLEDGMENTS

The authors are grateful for the technical discussion with Professor R. Itri about x-ray diffraction and to M. Aguilar by his technical support in x-ray diffraction. We acknowledge the support of DGAPA-UNAM and CONACYT grants IN110505 and 46778-F.

- ¹M. Daoud and C. E. Williams, *Soft Matter Physics* (Springer-Verlag, Berlin, 1999).
- ²F. Nallet, R. Laversanne, and D. Roux, *J. Phys. II* **3**, 487 (1993).
- ³T. Gulik-Krzywicki, *Curr. Opin. Colloid Interface Sci.* **2**, 132 (1997).
- ⁴H. W. Meyer and W. Richter, *Micron* **32**, 615 (2001).
- ⁵M. Almgren, K. Edwards, and G. Karlsson, *Colloids Surf.* **3**, 174 (2000).
- ⁶L. Belkoura, C. Stubenrauch, and R. Strey, *Langmuir* **20**, 4391 (2004).
- ⁷J. A. N. Zasadzinski, J. Schneir, J. Gurley, V. Elings, and P. K. Hansma, *Science* **239**, 1013 (1988).
- ⁸J. R. Bellare, H. T. Davis, L. E. Scriven, and Y. Talmon, *J. Electron Microsc. Tech.* **10**, 87 (1988).
- ⁹Y. Talmon, *Ber. Bunsenges. Phys. Chem.* **100**, 364 (1996).
- ¹⁰W. Jahn and R. Strey, *J. Phys. Chem.* **92**, 2294 (1988).
- ¹¹P. Alexandridis, U. Olsson, and B. Lindman, *Langmuir* **14**, 2627 (1998).
- ¹²K. Nakamoto, C. B. Mooney, and M. Iwatsuki, *Rev. Sci. Instrum.* **72**, 1445 (2001).
- ¹³H. E. Swanson and E. Tatge, *Natl. Bur. Stand. Circ. (U. S.)* **539** **1**, 23 (1953).
- ¹⁴C. Boissière, J. B. Brubach, A. Mermet, G. de Marzi, C. Bourgaux, E. Prouzet, and P. Roy, *J. Phys. Chem. B* **106**, 1032 (2002).
- ¹⁵R. Strey, R. Schomäcker, D. Roux, F. Nallet, and U. Olsson, *J. Chem. Soc., Faraday Trans.* **86**, 2253 (1990).